Studies of tetragonal $PbTiO_3$ subjected to uniaxial stress along the *c*-axis

2008 J. Phys.: Condens. Matter 20 175210

(http://iopscience.iop.org/0953-8984/20/17/175210)

J. Phys.: Condens. Matter **20** (2008) 175210 (5pp) doi:10.1088/0953-8984/20/17/175210

Studies of tetragonal $PbTiO_3$ subjected to uniaxial stress along the *c*-axis

Yifeng Duan[1], **Hongliang Shi**[1] **and Lixia Qin**[2]

[1] State Key Laboratory for Superlattices and Microstructures, Institute of Semiconductors, Chinese Academy of Sciences, PO Box 912, Beijing 100083, People's Republic of China
[2] Institute of Semiconductors, College of Physics and Electronics, Shandong Normal University, Jinan 250014, People's Republic of China

E-mail: yifeng@semi.ac.cn

Received 13 November 2007, in final form 27 February 2008
Published 3 April 2008
Online at stacks.iop.org/JPhysCM/20/175210

Abstract

Tetragonal $PbTiO_3$ under uniaxial stress along the *c*-axis is investigated from first-principles. The structural parameters, polarization, and squares of the lowest optical phonon frequencies for $E(1TO)$ and $A_1(1TO)$ modes at Γ show abrupt changes near a stress σ_c of 1.04 GPa, which is related to the dramatic change of elastic constant c_{33} resulting from the uniaxial stress applied along the *c*-axis. We also find that the uniaxial compressive stress could enhance the piezoelectric stress coefficients, whereas the uniaxial tensile stress could enhance the piezoelectric strain coefficients. It is also found that when the magnitude of uniaxial compressive stress σ_{33} is greater than 12 GPa, $PbTiO_3$ is transformed to the paraelectric tetragonal phase.

The ferroelectric $PbTiO_3$ (PTO) is well known as an end member of lead zirconate titanate, which has been used in many piezoelectronic devices, including acoustic and ultrasonic transducers, detectors, and actuators [1–4]. It is also one of the constituents for relaxor-PTO materials, such as $PbZn_{1/3}Nb_{2/3}O_3$–$PbTiO_3$ (PZN–PT) and $Pb(Mg_{1/3}Nb_{2/3}O_3)$–$PbTiO_3$ (PMN–PT) with very high electromechanical coupling properties and low dielectric loss [5]. The relaxor ferroelectrics are currently under intensive study [6–10], because their giant piezoelectric effects could revolutionize the field of piezoelectric devices. The complex mesoscopic ordering [11] in PZN–PT and PMN–PT greatly complicates their study from first-principles [12], but as the common compound for this class of materials, $PbTiO_3$ is supposed to play an important role in the observed behavior, and to study $PbTiO_3$ under uniaxial stress could be helpful for understanding the giant piezoelectric response of PZN–PT and PMN–PT.

$PbTiO_3$, as a prototype ferroelectric material, has a tetragonal, space group $P4mm$, ground state below its Curie temperature, with significant ferroelectric ionic displacements and a high *c*-axis strain of 6.5% [13]. The structure and properties of $PbTiO_3$ have been widely studied [14–23]. Under negative hydrostatic pressure, an enormous tetragonal strain is found, and the volume and atomic displacements change abruptly near a crossover pressure [24]. Samara *et al* [25] have demonstrated that hydrostatic pressure can reduce, and even annihilate for high enough value, ferroelectricity in perovskites, which is supported by Wu and Cohen's results [26]. It is known that ferroelectricity arises from the competition of short-range repulsions which favor the cubic phase and Coulomb forces which favor the ferroelectric phase [27]. As pressure increases, the short-range repulsions increase faster than the Coulomb forces. So far, there has been no previous work on the effects of uniaxial stress on the structural parameters, ferroelectricity, elasticity, and piezoelectric properties.

In this work, we have performed total energy as well as linear response calculations to study the effects of uniaxial stress on the structural parameters, polarization, Born effective charges, squares of the lowest optical phonon frequencies at Γ, elastic constants, and piezoelectric coefficients. The uniaxial stress is applied along the *c*-axis of the tetragonal $PbTiO_3$. The structural parameters, including volume, strains and atomic displacements, polarization, and squares of the lowest optical phonon frequencies show abrupt changes near a uniaxial stress σ_c, which is related to the dramatic change of elastic constant c_{33} resulting from the uniaxial stress along the *c*-axis. We also find that the uniaxial compressive stress could enhance the piezoelectric stress coefficients, whereas the uniaxial tensile

Table 1. Calculated elastic ($c_{\mu\nu}$) and piezoelectric (e_{iv}) constants of tetragonal $P4mm$ $PbTiO_3$. COS and CES represent the results calculated at optimized and experimental structures, respectively, which are compared with other theoretical and experimental data. $c_{\mu\nu}$ and e_{iv} are in GPa and C m^{-2}, respectively.

	Ours			
	COS	CES	Wu's[a]	Exp[b]
c_{11}	285	221	230	237
c_{12}	121	95.0	96.2	90
c_{13}	89.1	60.1	65.2	70
c_{33}	81.9	37.1	41.9	66
c_{44}	63.4	35.1	46.6	69
c_{66}	109	99.3	98.8	104
e_{31}	2.06	2.07	2.06	2.1
e_{33}	5.35	4.12	4.41	5.0
e_{15}	6.66	7.78	6.63	4.4

[a] Reference [26], LDA pseudopotential results at experimental structural parameters.
[b] Reference [37].

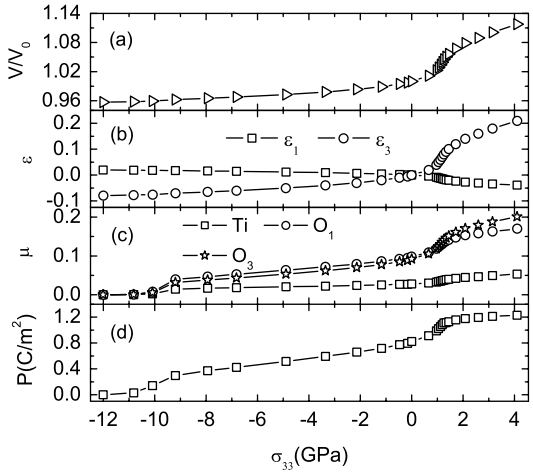

Figure 1. Uniaxial stress dependence of (a) normalized volume V/V_0, (b) strains ϵ_1 and ϵ_3, (c) atomic displacements μ along the c-axis (in c units), and (d) total polarization. The reference volume V_0 is 59.857 $Å^3$ for the case without strains. The O_1 (O_2) atom is on the xz (yz) face of the unit cell and the O_3 atom is located between two Ti atoms along the c-axis.

stress could enhance the piezoelectric strain coefficients. Moreover, it is found that $PbTiO_3$ shows paraelectric tetragonal symmetry when the magnitude of compressive stress σ_{33} is beyond 12 GPa.

Our calculations are performed within the local density approximation (LDA) to the density functional theory (DFT) as implemented in the plane-wave pseudopotential ABINIT package [28]. To obtain good convergence, the plane-wave energy cutoff is set to be 120 Ryd and the Brillouin zone integration is performed with $6 \times 6 \times 10$ **k**-meshpoints. The norm-conserving pseudopotentials are generated using the OPIUM program [29], and are rigorously tested against the all-electron full-potential linearized augmented plane-wave method [30]. The orbitals of Pb $5d^{10}6s^26p^2$, Ti $3s^23p^63d^24s^2$, and O $2s^22p^4$ are explicitly included as valence electrons. The dynamical matrices and Born effective charges are computed using the linear response theory of strain-type perturbations [31–33]. The polarization is calculated by the Berry-phase approach [34]. The LDA is used instead of the generalized gradient approximation (GGA) because the GGA catastrophically overestimates both equilibrium volume and strain for tetragonal $PbTiO_3$ [26, 35]. In the calculations, the piezoelectric strain coefficients $d_{iv} = \Sigma_{\mu=1}^{6} e_{i\mu} s_{\mu v}$, where **e** is the piezoelectric stress tensor and the elastic compliance tensor **s** is the reciprocal of the elastic stiffness tensor **c** (Roman indexes from 1 to 3, and Greek ones from 1 to 6).

To calculate the uniaxial stress along the c-axis, we apply a small strain in the [001] direction and conduct the structural optimization for the lattice vectors perpendicular to the c-axis and all the internal atomic positions. The minimization is done until the other two components of the stress tensor (i.e. σ_{11} and σ_{22}) are all smaller than 0.1 GPa. The strain is then increased step by step. Since σ_{11} (σ_{22}) $= \epsilon_1(c_{11} + c_{12}) + \epsilon_3 c_{13}$, when $\sigma_{33} \neq 0$, the elastic constants satisfy $\epsilon_3/\epsilon_1 \approx -(c_{11} + c_{12})/c_{13}$ [see below], where the strains ϵ_i are calculated using $\epsilon_1 = \epsilon_2 = (a - a_0)/a_0$ and $\epsilon_3 = (c - c_0)/c_0$, and a_0 and c_0 are lattice constants of the unstrained tetragonal structure. The LDA underestimates the volume, when $\sigma_{33} = 0$, our calculated equilibrium lattice constants are $a = 3.843$ Å, $c = 4.053$ Å with a c-axis tetragonal strain of 4.62% (the lattice constant of ideal cubic structure is 3.874 Å), which are less than the experimental lattice constants of 3.904 Å and 4.135 Å [36], respectively, and the experimental volume corresponds to a negative pressure $P_0 = -1.097$ GPa. We have calculated the elastic constants and piezoelectric coefficients at optimized and experimental lattice constants, respectively, which are compared with other theoretical [26] and experimental [37] data, as listed in table 1. For the optimized structure, the elastic constants are larger than those calculated at experimental structures, especially for c_{11}, c_{12}, c_{13} and c_{33}, due to the LDA underestimation of volume, but c_{44} and c_{66} are much closer to the experimental data. The calculated piezoelectric coefficients are in good agreement with the experimental data, except for e_{15}.

Figure 1 shows the optimized structural parameters and total polarization as a function of uniaxial stress σ_{33}. The structural parameters and polarization all show abrupt changes near the tensile stress $\sigma_c = 1.04$ GPa. The rapid increase of normalized volume V/V_0 results from the abrupt increase of strain ϵ_3. The strains ϵ_1 and ϵ_3 have opposite signs and satisfy abs$(\epsilon_1/\epsilon_3) < 0.5$. When $\sigma_{33} = 4.1$ GPa, $\epsilon_3 = 0.21$, corresponding to an enormous tetragonal strain. Note that the Pb atom is fixed at (0, 0, 0) during calculations. The displacements of Ti, O_1, and O_3 atoms all increase with increasing σ_{33}. When $\sigma_{33} < \sigma_c$, the displacement of the O_3 atom is smaller than that of the O_1 atom, whereas when $\sigma_{33} > \sigma_c$, the opposite is right, and at σ_c, the displacements of both types of oxygens are the same, suggesting that the oxygen cage could form a tetragonally strained octahedron [24]. The short Ti–O bond length along the c-axis remains almost constant, while the distance between decoupled Ti and O atoms also shows an abrupt increase at σ_c. As the magnitude of uniaxial compressive stress increases, the displacements of Ti, O_1, and

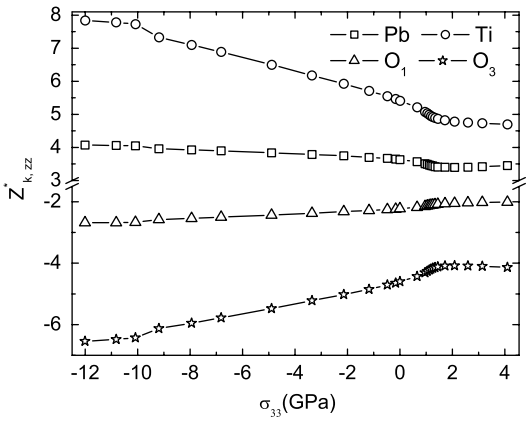

Figure 2. Born effective charges Z^*_{ZZ} of Pb, Ti, O_1, and O_3 as a function of uniaxial stress σ_{33}.

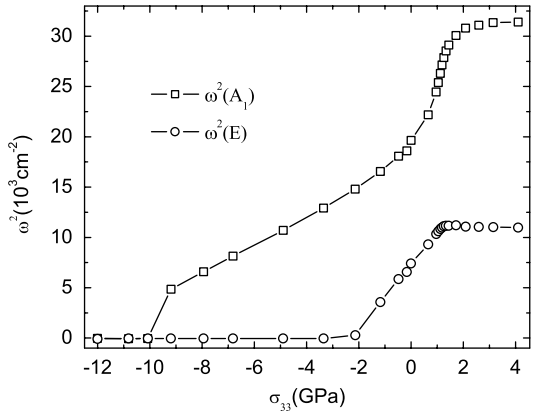

Figure 3. The squares of the lowest optical phonon frequencies for the $E(1\mathrm{TO})$ and $A_1(1\mathrm{TO})$ modes at Γ as a function of uniaxial stress σ_{33}.

Table 2. Calculated Born effective charges for tetragonal *P*4*mm* $PbTiO_3$ of the ground state at optimized structure.

Atom	Z^*_{xx}	Z^*_{yy}	Z^*_{zz}
Pb	3.85(3.74[a], 3.90[b])	3.85	3.63(3.52[a])
Ti	6.37(6.20[a], 7.06[b])	6.37	5.41(5.18[a])
O_1	−2.66(−2.61[a], −2.56[b])	−5.32(−5.18[a], −5.83[b])	−2.22(−2.16[a])
O_3	−2.24(−2.15[a])	−2.24	−4.60(−4.38[a])

[a] Reference [39].
[b] Reference [41], LDA pseudopotential results at experimental structural parameters.

O_3 atoms become smaller, and when the magnitude is beyond 12 GPa, all atoms are at their centrosymmetric positions of the unit cell and the lattice constants satisfy $c < a$, indicating that $PbTiO_3$ shows paraelectric tetragonal symmetry without polarization and piezoelectricity.

In ferroelectrics, the absolute polarizations of ferroelectric structures are generally determined from the change in polarization, relative to the related centrosymmetric reference structure, e.g. an ideal centrosymmetric perovskite structure with polarization equal to zero [38]. For the ground state $PbTiO_3$ at optimized structure, the spontaneous polarization is 0.82 C m^{-2}, which is in good agreement with another theoretical value of 0.88 C m^{-2} [39] and the experimental value of 0.75 C m^{-2} (295 K) [40]. The polarization is enhanced as uniaxial stress increases from negative to positive (see figure 1(d)), suggesting that the uniaxial tensile stress could enhance the ferroelectricity, whereas the uniaxial compressive stress would suppress it.

To get some insight into the polarization, we compute the Born effective charges Z^*. Since the polarization and atomic displacements are along the *c*-axis, only Z^*_{zz} of Pb, Ti, O_1 (O_2), and O_3 atoms contribute to the polarization, as shown in figure 2. We have examined the accuracy of our calculated results by comparison with other theoretical data [39, 41]. As summarized in table 2, good agreement is achieved. The Born effective charges Z^*_{zz} of Ti and O_3 atoms are anomalously large compared with their normal charges, suggesting the strong hybridization between O 2p and Ti 3d states [42–44]. Since the Pb–O and Ti–O orbital hybridization is sensitive to bond length [45, 46], the uniaxial compressive stress enhances the effective charges Z^*_{zz}, whereas the uniaxial tensile stress reduces them, and above σ_c, Z^*_{zz} of Pb, Ti, O_1, and O_3 atoms remain almost constant, which is related to the slow increase of polarization above σ_c. As uniaxial stress σ_{33} increases, atomic displacements are so strongly enhanced that the overall effect is the increase of polarization, even though the magnitudes of Z^*_{zz} decrease. The anomalous value of Z^*_{zz} is directly related to the large Coulomb forces [46]. As the magnitude of uniaxial compressive stress increases, the short-range repulsions increase faster than the Coulomb forces, and the short-range repulsions decrease faster than the Coulomb forces with increasing uniaxial tensile stress. The change of ferroelectricity is also emphasized by the uniaxial stress behavior of squares of the lowest optical phonon frequencies ω^2 at Γ for the $E(1\mathrm{TO})$ and $A_1(1\mathrm{TO})$ modes.

In tetragonal *P*4*mm* $PbTiO_3$, the $E(1\mathrm{TO})$ and $A_1(1\mathrm{TO})$ modes originate from the triply degenerate $F_{1\mu}(1\mathrm{TO})$ mode in the cubic phase, where the $E(1\mathrm{TO})$ mode is doubly degenerate [26]. The squares of such frequencies ω^2 at Γ also show abrupt changes near σ_c, as shown in figure 3. As the magnitude of uniaxial compressive stress σ_{33} increases, the squares always decrease, indicating the reduction, and finally disappearance, of the ferroelectric instability. It can also be concluded that tetragonal $PbTiO_3$ becomes more and more ferroelectric with increasing uniaxial tensile stress σ_{33}.

The abrupt variation of the structural parameters, polarization, and squares of the phonon frequencies near σ_c only appear when these properties are plotted as a function of uniaxial stress σ_{33}; the plot versus strain ϵ_3 does not show this anomalous behavior. To understand the relations between stresses and strains, we calculate the elastic stiffness and compliance constants (see figure 4). The elastic constant c_{33} is much larger than c_{13} for a broad range of stress. c_{33} first dramatically decreases with increasing σ_{33} below σ_c, and then slowly increases above σ_c, whereas the change of c_{13} is relatively small. The stress $\sigma_{33} = 2c_{13}\epsilon_1 + c_{33}\epsilon_3$ and the sign of σ_{33} is determined by c_{33} and ϵ_3. For two strains ϵ_3 with the same magnitude and different signs, the value of uniaxial

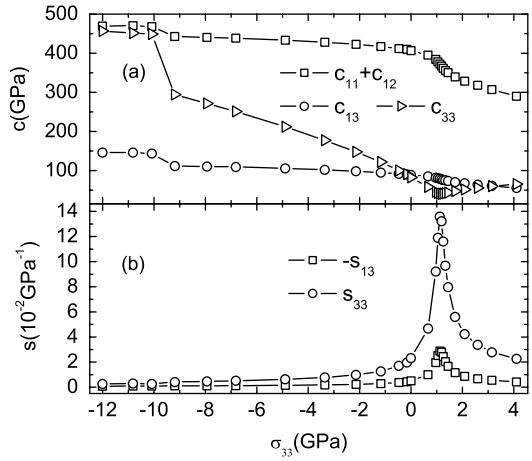

Figure 4. (a) Elastic stiffness and (b) elastic compliance constants as a function of uniaxial stress σ_{33}.

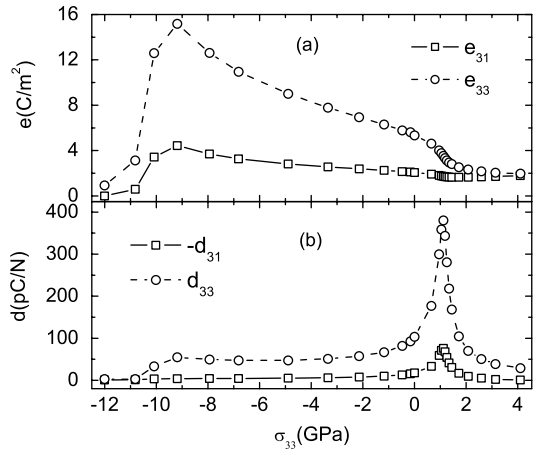

Figure 5. Uniaxial stress dependence of (a) piezoelectric stress coefficients (e_{31} and e_{33}) and (b) piezoelectric strain coefficients (d_{31} and d_{33}).

tensile stress is much smaller than the magnitude of uniaxial compressive stress, indicating that the structural parameters, polarization, and squares of the phonon frequencies are more sensitively affected by tensile stress than compressive stress.

Figure 5 shows the variation of piezoelectric stress and strain coefficients as a function of uniaxial stress, which are calculated by the linear response theory. The magnitudes of piezoelectric coefficients all first increase and then decrease with increasing σ_{33}. When $\sigma_{33} = -12$ GPa, piezoelectric coefficients are all equal to zero, which emphasizes the transition to paraelectric tetragonal phase. Piezoelectric stress (strain) coefficients reflect the relations between polarization and strain (stress), such as $d_{33} = \frac{\partial P}{\partial \sigma_{33}}$, which reflects the slope of the curve in figure 1(d). The maximum value of $d_{33} = 380.50$ pC N^{-1} corresponds to the abrupt increase of polarization at σ_c ($\epsilon_3 = 0.05$). When $\epsilon_3 = -0.07$ ($\sigma_{33} = -9.19$ GPa), the peak value of $e_{33} = 15.20$ C m^{-2} refers to the maximum slope when polarization is plotted as a function of strain ϵ_3, which has been verified by the relation between ϵ_3 and σ_{33} (see figure 1(b)). In the stress range near σ_c, $d_{31} \approx e_{33}s_{13}$, and $d_{33} \approx e_{33}s_{33}$, s_{13} and s_{33} all reach their extrema and s_{33} is much larger than the absolute value of s_{13} at σ_c (see figure 4(b)). Even though e_{33} decreases, the enhancement of s_{13} and s_{33} is so strong that d_{31} and d_{33} reach their extrema and d_{33} is much larger than the magnitude of d_{31} at σ_c. The polarization under uniaxial stress is always along the [001] direction. It is the change of the magnitude of polarization that leads to the enhancement of piezoelectricity. In Wu and Cohen's work [26], the giant piezoelectric effect of $PbTiO_3$ under hydrostatic pressure comes from noncollinear polarization rotation from [001] to [111] directions and occurs at the transition pressure from tetragonal to monoclinic phases, at which the total polarization changes continuously, whereas the polarization along the z-axis shows discontinuous change.

In summary, we have studied the structural parameters, polarization, Born effective charges, squares of the lowest optical phonon frequencies for the $E(1TO)$ and $A_1(1TO)$ modes at Γ, elastic constants, and piezoelectric coefficients of tetragonal $PbTiO_3$ under uniaxial stress along the c-axis using first-principles methods. The structural parameters, polarization, and squares of the phonon frequencies show abrupt changes near the uniaxial stress of 1.04 GPa, which could be explained by the change of elastic constants resulting from the uniaxial stress applied along the c-axis. The ferroelectricity is enhanced as the uniaxial stress increases from negative to positive. The maximum magnitudes of piezoelectric stress and strain coefficients appear at $\sigma_{33} = -9.19$ GPa and 1.04 GPa, respectively. It is also found that when the magnitude of uniaxial compressive stress σ_{33} is greater than 12 GPa, $PbTiO_3$ is in the paraelectric tetragonal phase.

Acknowledgments

The work is supported by the National Natural Science Foundation of China under Grant Nos 60325416, 60521001, and 90301007.

References

[1] Tanaka T 1982 *Ferroelectrics* **40** 167
[2] Sheppard L M 1992 *Cer. Bull.* **71** 85
[3] Lines M E and Glass A M 1979 *Principles and Applications of Ferroelectrics and Related Materials* (Oxford: Clarendon)
[4] Uchino K 1996 *Piezoelectric Actuators and Ultrasonic Motors* (Boston: Kluwer–Academic)
[5] Park S E and Shrout T R 1997 *J. Appl. Phys.* **82** 1804
[6] Kutnjak Z, Petzelt J and Blinc R 2006 *Nature* **441** 956
[7] Cohen R E 2006 *Nature* **441** 941
[8] Noheda B, Cox D E, Shirane G, Park S E, Cross L E and Zhong Z 2001 *Phys. Rev. Lett.* **86** 3891
[9] Wan Q, Chen C and Shen Y P 2005 *J. Appl. Phys.* **98** 024103
[10] Wan Q, Chen C and Shen Y P 2006 *J. Mater. Sci.* **41** 2993
[11] Egami T, Dmowski W, Akbas M and Davies P K 1998 *First-Principles Calculations for Ferroelectrics: Fifth Williamsburg Workshop* ed R E Cohen (Woodbury: AIP) pp 1–10
[12] Fu H and Cohen R E 2000 *Nature* **403** 281
[13] Shirane G 1956 *Acta Crystallogr.* **9** 131
[14] Burns G and Scott B A 1970 *Phys. Rev. Lett.* **25** 167

[15] García A and Vanderbilt D 1996 *Phys. Rev.* B **54** 3817
[16] Wu Z, Sághi-Szabó G, Cohen R E and Krakauer H 2005 *Phys. Rev. Lett.* **94** 069901
[17] Waghmare U V and Rabe K M 1997 *Phys. Rev.* B **55** 6161
[18] Sághi-Szabó G, Cohen R E and Krakauer H 1998 *Phys. Rev. Lett.* **80** 4321
[19] Posternak M, Resta R and Baldereschi A 1990 *Phys. Rev.* B **50** 8911
[20] Zhong W and Vanderbilt D 1995 *Phys. Rev. Lett.* **74** 2587
[21] Kuroiwa Y, Aoyagi S, Sawada A, Harada J, Nishibori E, Takata M and Sakata M 2001 *Phys. Rev. Lett.* **87** 217601
[22] Wu Z and Krakauer H 2003 *Phys. Rev.* B **68** 014112
[23] Kisi E H, Piltz R O, Forrester J S and Howard C J 2003 *J. Phys.: Condens. Matter* **15** 3631
[24] Tinte S, Rabe K M and Vanderbilt D 2003 *Phys. Rev.* B **68** 144105
[25] Samara G A, Sakudo T and Yoshimitsu K 1975 *Phys. Rev. Lett.* **35** 1767
[26] Wu Z and Cohen R E 2005 *Phys. Rev. Lett.* **95** 037601
[27] Cohen R E 1992 *Nature* **358** 136
[28] Gonze X, Beuken J-M, Caracas R, Detraux F, Fuchs M, Rignanese G-M, Sindic L, Verstraete M, Zerah G, Jollet F, Torrent M, Roy A, Mikami M, Ghosez Ph, Raty J-Y and Allan D C 2002 *Comput. Mater. Sci.* **25** 478
[29] Rappe A M, Rabe K M, Kaxiras E and Joannopoulos J D 1990 *Phys. Rev.* B **41** 1227
[30] Singh D J 1994 *Planewaves, Pseudopotential, and the LAPW Method* (Boston, MA: Kluwer–Academic)
[31] Gonze X and Lee C 1997 *Phys. Rev.* B **55** 10355
[32] Baroni S, de Gironcoli S, Dal Corso A and Giannozzi P 2001 *Rev. Mod. Phys.* **73** 515
[33] Hamann D R, Wu X, Rabe K M and Vanderbilt D 2005 *Phys. Rev.* B **71** 035117
[34] King-Smith R D and Vanderbilt D 1993 *Phys. Rev.* B **47** 1651
[35] Wu Z, Cohen R E and Singh D J 2004 *Phys. Rev.* B **70** 104112
[36] Glazer A M and Mabud S A 1978 *Acta Crystallogr.* B **34** 1065
[37] Cohen R E 2007 *Preprint* cond-mat/0702686
[38] Cockayne E and Burton B P 2004 *Phys. Rev.* B **69** 144116
[39] Sághi-Szabó G, Cohen R E and Krakauer H 1998 *Phys. Rev. Lett.* **80** 4321
[40] Gavrilyachenko V G *et al* 1970 *Sov. Phys.—Solid State* **12** 1203
[41] Zhong W, King-Smith R D and Vanderbilt D 1994 *Phys. Rev. Lett.* **72** 3618
[42] Ghosez Ph, Gonze X, Lambin P and Michenaud J-P 1995 *Phys. Rev.* B **51** 6765
[43] Ghosez Ph, Gonze X and Michenaud J-P 1998 *Ferroelectrics* **205** 206
[44] Posternak M, Resta R and Baldereschi A 1994 *Phys. Rev.* B **50** 8911
[45] Harrison W A 1980 *Electronic Structure and the Properties of Solids* (San Francisco, CA: Freeman)
[46] Ghosez P and Junquera J 2006 *Preprint* cond-mat/0605299